Generating a Topological Anomalous Hall Effect in a Nonmagnetic Conductor: An In-Plane Magnetic Field as a Direct Probe of the Berry Curvature

James H. Cullen,[1,2] Pankaj Bhalla,[3,2] E. Marcellina,[1,2,*,†] A. R. Hamilton,[1,2] and Dimitrie Culcer[1,2]
[1]School of Physics, The University of New South Wales, Sydney 2052, Australia
[2]Australian Research Council Centre of Excellence in Low-Energy Electronics Technologies, The University of New South Wales, Sydney 2052, Australia
[3]Beijing Computational Science Research Center, 100193 Beijing, China

(Received 15 November 2020; revised 22 April 2021; accepted 27 May 2021; published 21 June 2021)

We demonstrate that the Berry curvature monopole of nonmagnetic two-dimensional spin-$3/2$ holes leads to a novel Hall effect linear in an applied in-plane magnetic field $B_{\parallel}$. Remarkably, all scalar and spin-dependent disorder contributions vanish to leading order in $B_{\parallel}$, while there is no Lorentz force and hence no ordinary Hall effect. This purely intrinsic phenomenon, which we term the anomalous planar Hall effect (APHE), provides a direct transport probe of the Berry curvature accessible in all p-type semiconductors. We discuss experimental setups for its measurement.

DOI: 10.1103/PhysRevLett.126.256601

Introduction.—Topological responses are ubiquitous in solids but isolating them is a difficult task. Quantized responses, such as the quantum Hall and quantum spin-Hall effects [1–4], provide a clear fingerprint of topology, yet these have been observed only in one-dimensional (1D) systems and are intimately connected with the existence of edge states [1–8]. In 2D and 3D conductors a hotly debated topological response occurs in the anomalous Hall effect (AHE), where the Berry curvature mechanism has never been detected unambiguously. Originally observed in ferromagnets, the AHE was shown to exist in paramagnetic materials as well [9], where the Berry curvature contribution is strong. Although the Berry curvature can lead to a quantized response [5–7,9–15] such quantization is impossible to observe in practice for two main reasons. First, the dispersion involves an even number of Zeeman-split Kramers pairs that make opposite contributions, yielding a nonuniversal conductivity that is often density dependent [12,16–18]. Second, disorder is unavoidable [19,20]: scalar disorder reduces and occasionally wipes out the Berry curvature contribution, while spin-dependent scattering overwhelms the remainder. The manifold contributions to the AHE have been debated for three quarters of a century [9–12,18,19,21–31], and controversy surrounds it even as it opens new avenues of research [32–37].

In this Letter we provide a smoking gun in this lengthy debate by identifying a system in which the Berry curvature can be unambiguously detected in transport. We show that a Hall effect is generated in a 2D heavy-hole system grown along a low-symmetry direction when an in-plane magnetic field $B_{\parallel}$ is applied. In the absence of an out-of-plane magnetic field and therefore of a Lorentz force, there is no ordinary Hall effect. Instead, an anomalous Hall effect occurs due to the finite Berry curvature of the spin-$3/2$ hole system. The gap in the dispersion that enables the Hall response is opened by a shear Zeeman term in the Lande g tensor [38,39]. Our central result is the Hall conductivity σ_{xy} linear in $B_{\parallel}$, shown in Figs. 1 and 2 and expected from the Onsager relations. We refer to this phenomenon as the anomalous planar Hall effect (APHE). Its origins are intrinsic and topological: remarkably, neither scalar nor extrinsic spin-orbit scattering contributes to leading order in $B_{\parallel}$. Because the equilibrium system is not magnetized the effect is tunable *in situ* by altering the magnetic field orientation. It is observable in state-of-the-art hole samples, which have been developing at a brisk pace. Part of the motivation stems from quantum computing applications

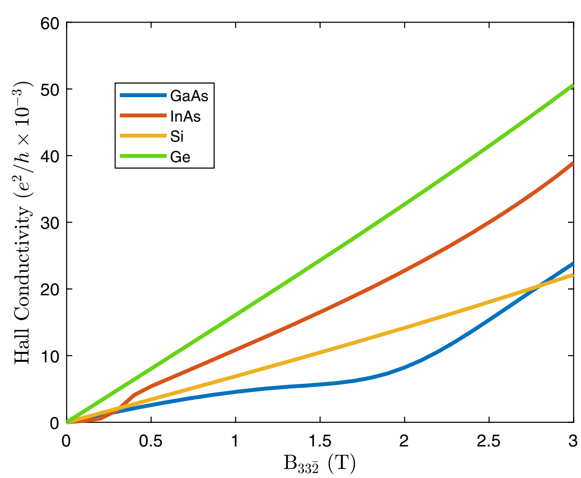

FIG. 1. Intrinsic Hall conductivity vs in-plane magnetic field for different materials, for a symmetrically biased quantum well grown along (113) of width 20 nm. The Fermi energy is 5 meV, the carrier densities $\approx$5–25 $\times 10^{10}$ cm^{-2}.

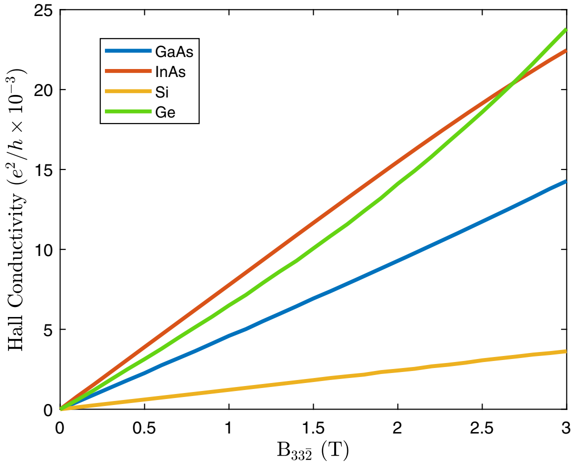

FIG. 2. Intrinsic Hall conductivity versus in-plane magnetic field for an asymmetrically biased well $\|$ (113) with top gate field $E_z = 5$ MV/m and well width of 20 nm. The Fermi energy is 5 meV, the carrier densities ≈ 5–25×10^{10} cm^{-2}.

[40–57], in which holes are actively investigated [58–60], as well as from their large spin-orbit coupling [61–63] and unconventional spin-3/2 nature [64–77], leading to transport characteristics with no counterpart in spin-1/2 electron systems [78–82].

We consider a 2D hole gas grown along (113). Our findings hold for a multitude of low-symmetry growth directions, and (113) is chosen as an example. The ground state is the heavy hole manifold, where heavy holes have spin projection $\pm 3/2$ onto the quantization axis, perpendicular to the plane. At normal transport densities the light hole manifold is not occupied. Our results are obtained using the Luttinger Hamiltonian rotated along the growth direction (113) with the vertical confinement modeled by the Bastard wave function, given in the Supplemental Material [83]. Nevertheless, the underlying physics can be understood from the effective Hamiltonian for the lowest heavy hole subband $H_{hh} = \varepsilon_{0\boldsymbol{k}} + H_s + H_c = \varepsilon_{0\boldsymbol{k}} + (\hbar/2)\boldsymbol{\sigma}\cdot\boldsymbol{\Omega}_{\boldsymbol{k}}$, where $\varepsilon_{0\boldsymbol{k}} = \hbar^2 k^2/(2m^*)$ and $\boldsymbol{\sigma}$ is the vector of Pauli spin matrices; m^* is the heavy-hole in-plane effective mass and $\boldsymbol{k}$ is the in-plane wave vector. The term H_s captures the leading contributions to the Rashba and Zeeman effects, which stem from the spherical terms in the Luttinger Hamiltonian [84–90], as well as the out-of-plane Zeeman term, which stems from the cubic symmetry of diamond and zinc blende lattices [39]. Written in full,

$$
\begin{aligned}
H_s = {}& i\alpha(\sigma_+ k_-^3 - \sigma_- k_+^3) + \Delta_1(\sigma_+ B_- k_-^2 + \sigma_- B_+ k_+^2) \\
&+ \Delta_2(\sigma_+ B_+ k_-^4 + \sigma_- B_- k_+^4) + \Delta_3 k^2(\sigma_+ B_+ + \sigma_- B_-) \\
&+ \Delta_4(\sigma_+ B_- k_+^2 + \sigma_- B_+ k_-^2) + \Delta_{zx}\sigma_z B_x,
\end{aligned} \tag{1}
$$

where α is the Rashba spin-orbit constant in the spherical approximation; $k_\pm = k_x \pm i k_y$; $B_\pm = B_x \pm i B_y$; and Δ_1, Δ_2, Δ_3, and Δ_4 are effective Lande g factors [89–91], with Δ_3 and Δ_4 present only in asymmetric wells [89,90]. The shear Zeeman term $\Delta_{zx}\sigma_z B_x$ is vital [38,39], yielding an out-of-plane Zeeman splitting in response to an in-plane magnetic field that henceforth we assume to be $\|\hat{\boldsymbol{x}}$, where $\hat{\boldsymbol{x}}\|(33\bar{2})$. Cubic symmetry leads to the following additional spin-orbit terms:

$$
\begin{aligned}
H_c = {}& \eta_1 \sigma_z k_y + \eta_2 \sigma_z k_y (11 k_y^2 - 49 k_x^2) \\
&+ i\eta_3(\sigma_+ k_- - \sigma_- k_+).
\end{aligned} \tag{2}
$$

Here η_1 has contributions from the Dresselhaus terms $\propto C_D, B_{D1}$ in Ref. [88], $\eta_2 \propto B_{D1}$, while η_3 has contributions from both Dresselhaus and cubic-symmetry terms. Dresselhaus terms are absent in diamond lattices such as Si and Ge but are noticeable in zinc blende materials such as GaAs and InAs. In the Supplemental Material [83] we find that diamond and zinc blende quantum wells have comparable Rashba splittings at realistic transport densities. All spin-dependent interactions can be incorporated into an effective field $\boldsymbol{\Omega}_{\boldsymbol{k}}$. The eigenvalues of H_{hh} are $\varepsilon_{\boldsymbol{k}\pm} = \varepsilon_{0\boldsymbol{k}} \pm \hbar|\Omega_{\boldsymbol{k}}|$. We assume $\Omega_F \tau \gg 1$, with Ω_F the value of $\boldsymbol{\Omega}_{\boldsymbol{k}}$ on the Fermi surface and τ the momentum relaxation time.

We focus first on the Hall current due to H_s, which provides the dominant contribution. The effects of the much smaller terms contained in H_c [88], as well as disorder, are discussed in the closing section. The Zeeman term for heavy holes also includes the terms $\propto B_\|^3$, yet these are three orders of magnitude smaller than the $B_\|$-linear terms above, becoming important only for $B_\| \geq 30$ T. The coefficients in Eqs. (1) and (2) are functions of k and decrease strongly at larger wave vectors. Such momentum-dependent Zeeman terms with different winding numbers are likewise specific to heavy holes, since these correspond to the $\pm 3/2$ projection of the hole spin-3/2 onto the quantization axis [81]. They have no counterpart in electron systems. In our evaluations of the Hall conductivity for Figs. 1 and 2 this k dependence is circumvented by using the full 4×4 Luttinger Hamiltonian.

Unlike the ordinary Hall effect driven by the Lorentz force, the charge dynamics here originate in the spin locking to the wave vector. As a hole is accelerated longitudinally its wave vector changes and it experiences a different spin-orbit field. As a result of this the spin undergoes a rotation, which in turn produces a change in the wave vector that is perpendicular to the longitudinal motion, in other words, a Hall current. The intrinsic Hall conductivity, derived below, is given by $\sigma_{xy}^0 = -(e^2/h)\int d^2k/(2\pi)\mathcal{F}_z^n$, where the Berry curvature of subband n is $\boldsymbol{\mathcal{F}}_n = -\mathrm{Im}\langle \partial u_n/\partial \mathbf{k}| \times |\partial u_n/\partial \mathbf{k}\rangle$, with u_n the lattice-periodic Bloch wave function, whose role is played here by the envelope function. The full effect as a

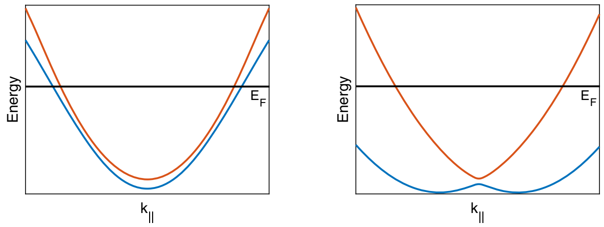

FIG. 3. The in-plane dispersion of the two spin-split HH subbands for a 2D hole gas grown along (113) with an in-plane magnetic field. (a) Symmetric well. (b) Asymmetric well.

function of magnetic field, including its material dependence, is shown in Fig. 1 for a symmetric well and in Fig. 2 for a strongly asymmetric well, in which the Rashba interaction dominates. The form and behavior of the Hall conductivity are understood by noting that (i) the shear Zeeman term opens a gap, which makes the Berry curvature nonzero; (ii) the spin-split bands have different Fermi wave vectors; and (iii) the sign of the Berry curvature is determined by the winding direction of the spin-orbit field $\mathbf{\Omega}_{\boldsymbol{k}}$, with the Rashba, in-plane Zeeman and the Dresselhaus terms all yielding the same sign. However, for different low symmetry growth directions these contributions can yield different signs. We first provide a pedagogical analytical explanation for these two limiting cases: a symmetric well with a single in-plane Zeeman term expected to dominate at small densities and a strongly asymmetric well. For simplicity we use constant coefficients to derive approximate analytical expressions for σ_{xy}, noting that this pedagogical approach is restricted to very small densities and magnetic fields. The dispersions for these two cases are sketched in Fig. 3.

In a symmetric well in Si and Ge, given that there is no *a priori* spin-orbit coupling, the Berry curvature is initially zero. When the in-plane magnetic field is applied, the Zeeman terms $\propto \Delta_1, \Delta_2$ give rise to a nonzero Berry curvature at each $\boldsymbol{k}$, while the Zeeman term $\propto \Delta_{zx}$ opens a gap in the spectrum. Interestingly, the Berry curvature itself is independent of $B_{||}$, although it depends explicitly on the in-plane and out-of-plane g factors. Since the heavy-hole subband is now spin split by the out-of-plane Zeeman interaction there are two different Fermi wave vectors. The difference between them is linear in the magnetic field at low fields, as shown in the Supplemental Material [83]; hence the conductivity is linear in $B_{||}$. With only the Δ_1 and Δ_{zx} terms, the Hall conductivity reads

$$\sigma_{xy} = \frac{e^2}{h} B_{||} \left[\frac{8\Delta_{zx}\Delta_1^2 m^{*2}\epsilon_F}{\hbar^4 (\Delta_{zx}^2 + \frac{4\Delta_1^2 m^{*2}\epsilon_F^2}{\hbar^4})} \right], \tag{3}$$

which increases monotonically with $B_{||}$. In GaAs and InAs, on the other hand, the Dresselhaus terms cause σ_{xy} to be nonlinear at small fields but their contribution to the Berry curvature is eventually overwhelmed by the in-plane Zeeman terms as $B_{||}$ increases.

In an asymmetric well the Berry curvature is likewise zero in the absence of the out-of-plane Zeeman interaction. Nevertheless, the heavy hole subband is already spin split by the strong Rashba spin-orbit interaction even before the magnetic field is turned on, so that there is a sizable difference between the two Fermi wave vectors. The Rashba interaction overwhelms all other terms, as shown recently [88]; hence the plots for the asymmetric well increase monotonically for all materials. When the Zeeman term $\propto \Delta_{zx}$ opens a gap a significant Hall current emerges. With only the Rashba and Δ_{zx} terms, the Hall conductivity takes the form

$$\sigma_{xy} = \frac{e^2}{h} B_{||} \left(\frac{3\Delta_{zx}}{2\alpha} \right) \left(\frac{1}{k_{F+}^3} - \frac{1}{k_{F-}^3} \right). \tag{4}$$

The Fermi wave vectors $k_{F\pm} \approx ((2m^*\epsilon_F/\hbar^2) \mp (4\sqrt{2}\alpha m^{*(5/2)}\epsilon_F^{3/2}/\hbar^5))^{1/2}$ differ due to the Rashba interaction, while their magnetic field dependence is negligible. Because of this, when the spin-orbit energy $\Omega_F > \Delta_{zx}B_x$ but is still much less than the kinetic energy, σ_{xy} is approximately independent of spin-orbit strength. This insight is more general than just the Rashba case and explains the relative smallness of the effect and its comparable size in all materials studied. The APHE is driven by the cubic-symmetry and bulk Zeeman terms, which are strongest in InAs and Ge. In a realistic sample we expect $\rho_{xy} \sim 100$–$500\ \mu\Omega$.

Experimental measurement.—A schematic of an experimental setup that could be used to measure the APHE is shown in Fig. 4. To identify the Berry curvature terms experimentally, one can start with a (113) quantum well with a top and bottom gate that enables full control of the Rashba interaction [38,92,93] and apply an in-plane magnetic field to introduce the Zeeman interactions (1). The Berry curvature terms can be detected through the Hall voltage, which depends directly on σ_{xy}. As the magnetic field is rotated in the plane the Hall current will disappear, since $\Delta_{zy} = 0$, enabling one to turn the APHE on and off *in situ*. The fact that heavy holes along (113) do not exhibit a Zeeman response to a magnetic field $\|\hat{\boldsymbol{y}}$ reflect their weak interaction with an in-plane magnetic field, which vanishes for structures grown along the main crystal axes. As the magnetic field is rotated out of the plane the APHE will give way to the ordinary Hall effect.

Methodology.—The full Hamiltonian $H = H_{hh} + H_E + U$. The driving electric field $\boldsymbol{E}\|\hat{\boldsymbol{y}}$ is contained in $H_E = e\boldsymbol{E}\cdot\hat{\boldsymbol{r}}$. The scattering potential $U(\boldsymbol{r}) = \sum_I \bar{U}(\boldsymbol{r} - \boldsymbol{R}_I)$; includes both scalar and extrinsic spin-orbit scattering [94], where $\boldsymbol{R}_I$ indexes the random locations of impurities; and the scattering potential due to a single impurity is denoted by

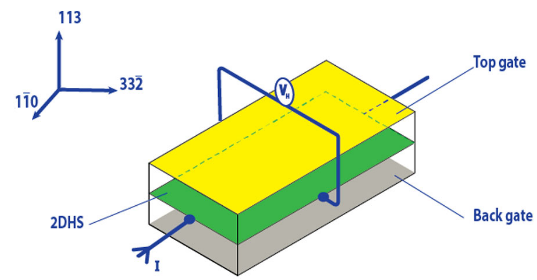

FIG. 4. Experimental setup for measuring the APHE. A magnetic field $\|(33\bar{2})$ will cause a Hall current. Rotating it to $(1\bar{1}0)$ will cause the Hall current to disappear.

$\bar{U}(\boldsymbol{r})$. In Fourier space, $\bar{U}_{\boldsymbol{kk}'} = \mathcal{U}_{\boldsymbol{kk}'}\mathbb{1} + \mathcal{V}_{\boldsymbol{kk}'}$, where $\mathcal{U}_{\boldsymbol{kk}'}$ represents a matrix element between plane waves, and $\mathcal{V}_{\boldsymbol{kk}'} = -(i\lambda/2)\boldsymbol{\sigma}\cdot(\boldsymbol{\omega}_{\boldsymbol{k}}\times\boldsymbol{k}' - \boldsymbol{\omega}_{\boldsymbol{k}'}\times\boldsymbol{k})\mathcal{U}_{\boldsymbol{kk}'}$, where $\boldsymbol{\omega}_{\boldsymbol{k}} = k^3(\cos 3\theta, \sin 3\theta, 0)$, assuming $\lambda k_F^4 \ll 1$. Because the Rashba Hamiltonian is derived from the Luttinger Hamiltonian in the spherical approximation it has the same form along (113) as along (001), and thus the extrinsic spin-orbit scattering term has the same form as in Ref. [94]. As written in the Pauli basis, the spin-dependent term $\mathcal{V}_{\boldsymbol{kk}'}$ points out of the plane. We note that λ for holes has not been determined quantitatively. We consider short-range scattering off uncorrelated impurities, with the average of $\langle \boldsymbol{k}n|\hat{U}|\boldsymbol{k}'n'\rangle\langle\boldsymbol{k}'n'\hat{U}|\boldsymbol{k}n\rangle$ over impurity configurations $n_i|\bar{U}^{nn'}_{\boldsymbol{kk}'}|^2/V$, where n_i is the impurity density and V the crystal volume.

We derive a quantum kinetic equation as described in Refs. [20,95]. The density matrix ρ is found in the basis $\{\boldsymbol{k}n\}$, where n represents the band index. To determine the charge current we require $f_{\boldsymbol{k}}$, the part of the density matrix diagonal in wave vector, because the current operator is diagonal in $\boldsymbol{k}$. From the quantum Liouville equation, $\partial\rho/\partial t + (i/\hbar)[H,\rho] = 0$, we obtain the following kinetic equation describing the time evolution of $f_{\boldsymbol{k}}$:

$$\frac{\partial f_{\boldsymbol{k}}}{\partial t} + \frac{i}{\hbar}[H_{hh}, f_{\boldsymbol{k}}] + \hat{J}(f_{\boldsymbol{k}}) = \mathcal{D}_{E,\boldsymbol{k}}, \tag{5}$$

where the scattering term in the Born approximation

$$\hat{J}(f_{\boldsymbol{k}}) = \langle\frac{1}{\hbar^2}\int_0^\infty dt'[\hat{U}, e^{-\frac{iH_{hh}t'}{\hbar}}[\hat{U}, \hat{f}(t)]e^{\frac{iH_{hh}t'}{\hbar}}]\rangle, \tag{6}$$

and the driving term $\mathcal{D}_{E,\boldsymbol{k}} = (e\boldsymbol{E}/\hbar)\cdot(Df_{0\boldsymbol{k}}/D\boldsymbol{k})$. The covariant derivative $Df_{0\boldsymbol{k}}/D\boldsymbol{k} = \partial f_{0\boldsymbol{k}}/\partial\boldsymbol{k} - i[\mathcal{R}_{\boldsymbol{k}}, f_{0\boldsymbol{k}}]$ arises from the $\boldsymbol{k}$ dependence of the basis functions. The Berry connection matrix elements $\mathcal{R}^{mm'}_{\boldsymbol{k}} = \langle u^m_{\boldsymbol{k}}|i(\partial u^{m'}_{\boldsymbol{k}}/\partial\boldsymbol{k})\rangle$, with $m \neq m'$ necessarily, are interband matrix elements of the position operator, which also appear in the current density operator $\boldsymbol{j} = -(e/\hbar)DH_{hh}/D\boldsymbol{k}$. In an external electric field one may decompose $f_{\boldsymbol{k}} = f_{0\boldsymbol{k}} + f_{E\boldsymbol{k}}$, where $f_{0\boldsymbol{k}}$ is the equilibrium density matrix and $f_{E\boldsymbol{k}}$ is a correction to first order in the electric field. The equilibrium density matrix is $f_{0\boldsymbol{k}} = (1/2)[(f_{\boldsymbol{k}+} + f_{\boldsymbol{k}-})\mathbb{1} + \tilde{\sigma}_z(f_{\boldsymbol{k}+} - f_{\boldsymbol{k}-})]$, where $f_{\boldsymbol{k}\pm}$ represent the Fermi-Dirac distributions over subband energies $\varepsilon_{\boldsymbol{k}\pm}$, and the tilde in $\tilde{\sigma}_z$ denotes the basis of eigenstates of the band Hamiltonian. In linear response one may replace $f_{\boldsymbol{k}} \to f_{0\boldsymbol{k}}$ in the driving term $\mathcal{D}_{E,\boldsymbol{k}}$. With $f_{0\boldsymbol{k}}$ known and $\mathcal{D}_{E,\boldsymbol{k}}$ on the right-hand side of Eq. (5), we obtain $f_{E\boldsymbol{k}}$. By taking the trace with the current operator, the longitudinal and transverse components of the current are found. The off-diagonal part of the density matrix contains the intrinsic term $S^{mm'}_{E\boldsymbol{k}} = -i\hbar\mathcal{P}[D^{mm'}_{E\boldsymbol{k}}(\varepsilon^m_{\boldsymbol{k}} - \varepsilon^{m'}_{\boldsymbol{k}})]$, with $\mathcal{P}$ the principal part, and this yields directly the intrinsic Hall conductivity as introduced above.

Disorder contributions.—Disorder is responsible for a complex series of contributions to the Hall conductivity, which in related models tend to reduce the Hall effect or cancel it altogether [19,20]. Disorder contributions fall into two categories: those stemming from scalar disorder and those from spin-dependent disorder. The former exist because of interband coherence induced by the electric field, which causes even scalar disorder to contribute to the Hall effect through an anomalous driving term

$$D'^{mm''}_{E\boldsymbol{k}} = \frac{\pi n_i}{\hbar}\sum_{m'\boldsymbol{k}'}\mathcal{U}^{mm'}_{\boldsymbol{kk}'}\mathcal{U}^{m'm''}_{\boldsymbol{k}'\boldsymbol{k}}[(n^m_{E\boldsymbol{k}} - n^{m'}_{E\boldsymbol{k}'})\delta(\varepsilon^m_{\boldsymbol{k}} - \varepsilon^{m'}_{\boldsymbol{k}'}) + (n^{m''}_{E\boldsymbol{k}} - n^{m'}_{E\boldsymbol{k}})\delta(\varepsilon^{m''}_{\boldsymbol{k}} - \varepsilon^{m'}_{\boldsymbol{k}'})]. \tag{7}$$

Here we have singled out the band-diagonal term in the density matrix, $n^{mm'}_{E\boldsymbol{k}} \propto \delta^{mm'}$. To find $D'^{mm''}_{E\boldsymbol{k}}$, we first solve for $n_{E\boldsymbol{k}}$, feed it into the scattering term Eq. (6), and take the band off-diagonal part. When calculated explicitly this contribution is identically zero for both symmetric and strongly asymmetric wells for both the spherical Rashba interaction and the Zeeman terms.

The spin-dependent disorder term $\mathcal{V}_{\boldsymbol{kk}'}$ gives rise to four contributions: skew scattering, side jump, anomalous spin precession, and the anomalous scattering term. These are described in detail in Ref. [94] for the spin-Hall effect, and the method here is exactly analogous. Because of the large winding numbers involved the anomalous spin precession and the anomalous scattering terms are zero for holes, while skew scattering and side jump contribute only to order $B^3_\parallel$. These terms cause hole up and down spins to scatter predominantly in different directions, but after scattering the spins process under the action of the band structure spin-orbit field, so their contribution to the Hall effect is washed out to first order in $B_\parallel$. We also find the contribution from $J_\lambda(S_{E\parallel})$ to be imaginary. The extrinsic term linear in $B_\parallel$ vanishes because (i) the Zeeman terms and the extrinsic spin-orbit effective field have large winding numbers and (ii) the extrinsic spin-orbit field points out of the plane. Consequently, with the Rashba interaction evaluated in the spherical approximation, and in the absence of Dresselhaus terms, there are no disorder contributions to the APHE.

We investigate the contributions due to the Dresselhaus and cubic-symmetry Rashba term. The term $\propto \eta_3$ in Eq. (2) is linear in the wave vector; therefore its contribution to the intrinsic part of the Hall current is canceled exactly by the scalar disorder term in the same way as the linear Rashba term in electron systems [19,20]. It does not contribute to the extrinsic signal because it generates a spin-orbit field that is purely in the plane. The Dresselhaus terms make a contribution to the Berry curvature, which is noticeable only in symmetric wells, as discussed above. Since the Dresselhaus spin-orbit field $\propto \eta_1, \eta_2$ points out of the plane, it does not contribute to the extrinsic signal through the anomalous scattering term $J_{\Omega\lambda}(n_{E\parallel})$. It does not contribute to the Hall current through the anomalous driving term either. The only way a nonzero contribution to the current can emerge is through products of the Dresselhaus terms and cubic symmetry terms, which will then be multiplied by the small parameter $\lambda k_F^4 \ll 1$. Therefore, in Si and Ge the extrinsic contribution to the APHE vanishes altogether, while in InAs and GaAs it is negligibly small.

In summary, we have shown that low-symmetry growth hole nanostructures exhibit a purely Berry curvature–driven Hall effect in response to an in-plane magnetic field. The APHE may open new pathways in the electrical operation of spin qubits and spin-orbit torques.

This work was funded by the Australian Research Council Centre of Excellence in Future Low-Energy Electronics Technologies. P. B. acknowledges the National Key Research and Development Program of China Grant No. 2017YFA0303400, China Postdoctoral Science Foundation Grant No. 2019M650461, and NSAF China Grant No. U1930402 for financial support. We thank Assa Auerbach, Abhisek Samanta, Daniel Arovas, John Schliemann, and Michael Fuhrer for helpful discussions.

*emarcellina@ntu.edu.sg

†Present address: School of Physical and Mathematical Sciences, Nanyang Technological University, 21 Nanyang Link, Singapore 637371.

[1] K. v. Klitzing, G. Dorda, and M. Pepper, Phys. Rev. Lett. **45**, 494 (1980).
[2] B. A. Bernevig, T. L. Hughes, and S.-C. Zhang, Science **314**, 1757 (2006).
[3] M. König, S. Wiedmann, C. Brüne, A. Roth, H. Buhmann, L. W. Molenkamp, X.-L. Qi, and S.-C. Zhang, Science **318**, 766 (2007).
[4] D. Culcer, A. C. Keser, Y. Li, and G. Tkachov, 2D Mater. **7**, 022007 (2020).
[5] C.-Z. Chang, J. Zhang, X. Feng, J. Shen, Z. Zhang, M. Guo, K. Li, Y. Ou, P. Wei, L.-L. Wang, Z.-Q. Ji, Y. Feng, S. Ji, X. Chen, J. Jia, X. Dai, Z. Fang, S.-C. Zhang, K. He, Y. Wang, L. Lu, X.-C. Ma, and Q.-K. Xue, Science **340**, 167 (2013).
[6] C.-Z. Chang, W. Zhao, D. Y. Kim, H. Zhang, B. A. Assaf, D. Heiman, S.-C. Zhang, C. Liu, M. H. W. Chan, and J. S. Moodera, Nat. Mater. **14**, 473 (2015).
[7] A. J. Bestwick, E. J. Fox, X. Kou, L. Pan, K. L. Wang, and D. Goldhaber-Gordon, Phys. Rev. Lett. **114**, 187201 (2015).
[8] J. L. Collins, A. Tadich, W. Wu, L. C. Gomes, J. N. B. Rodrigues, C. Liu, J. Hellerstedt, H. Ryu, S. Tang, S.-K. Mo, S. Adam, S. A. Yang, M. S. Fuhrer, and M. T. Edmonds, Nature (London) **564**, 390 (2018).
[9] D. Culcer, A. H. MacDonald, and Q. Niu, Phys. Rev. B **68**, 045327 (2003).
[10] M. Onoda and N. Nagaosa, J. Phys. Soc. Jpn. **71**, 19 (2002).
[11] F. D. M. Haldane, Phys. Rev. Lett. **93**, 206602 (2004).
[12] N. A. Sinitsyn, A. H. MacDonald, T. Jungwirth, V. K. Dugaev, and J. Sinova, Phys. Rev. B **75**, 045315 (2007).
[13] R. Yu, W. Zhang, H.-J. Zhang, S.-C. Zhang, X. Dai, and Z. Fang, Science **329**, 61 (2010).
[14] S. Qi, Z. Qiao, X. Deng, E. D. Cubuk, H. Chen, W. Zhu, E. Kaxiras, S. B. Zhang, X. Xu, and Z. Zhang, Phys. Rev. Lett. **117**, 056804 (2016).
[15] C.-X. Liu, S.-C. Zhang, and X.-L. Qi, Annu. Rev. Condens. Matter Phys. **7**, 301 (2016).
[16] T. Jungwirth, Q. Niu, and A. H. MacDonald, Phys. Rev. Lett. **88**, 207208 (2002).
[17] T. S. Nunner, N. A. Sinitsyn, M. F. Borunda, V. K. Dugaev, A. A. Kovalev, A. Abanov, C. Timm, T. Jungwirth, J.-I. Inoue, A. H. MacDonald, and J. Sinova, Phys. Rev. B **76**, 235312 (2007).
[18] N. Nagaosa, J. Sinova, S. Onoda, A. H. MacDonald, and N. P. Ong, Rev. Mod. Phys. **82**, 1539 (2010).
[19] J.-i. Inoue, T. Kato, Y. Ishikawa, H. Itoh, G. E. W. Bauer, and L. W. Molenkamp, Phys. Rev. Lett. **97**, 046604 (2006).
[20] D. Culcer, A. Sekine, and A. H. MacDonald, Phys. Rev. B **96**, 035106 (2017).
[21] J. M. Luttinger, Phys. Rev. **112**, 739 (1958).
[22] J. Smit, Physica (Amsterdam) **24**, 39 (1958).
[23] L. Berger, Phys. Rev. B **2**, 4559 (1970).
[24] P. Nozières and C. Lewiner, J. Phys. (Paris) **34**, 901 (1973).
[25] A. Crépieux and P. Bruno, Phys. Rev. B **64**, 014416 (2001).
[26] V. K. Dugaev, A. Crepieux, and P. Bruno, Phys. Rev. B **64**, 104411 (2001).
[27] S. Onoda, N. Sugimoto, and N. Nagaosa, Phys. Rev. B **77**, 165103 (2008).
[28] N. A. Sinitsyn, J. Phys. Condens. Matter **20**, 023201 (2008).
[29] A. A. Kovalev, Y. Tserkovnyak, K. Vyborny, and J. Sinova, Phys. Rev. B **79**, 195129 (2009).
[30] S. A. Yang, H. Pan, Y. Yao, and Q. Niu, Phys. Rev. B **83**, 125122 (2011).
[31] K. Nomura and N. Nagaosa, Phys. Rev. Lett. **106**, 166802 (2011).
[32] D. Culcer and S. Das Sarma, Phys. Rev. B **83**, 245441 (2011).
[33] I. A. Ado, I. A. Dmitriev, P. M. Ostrovsky, and M. Titov, Europhys. Lett. **111**, 37004 (2015).
[34] I. A. Ado, I. Dmitriev, P. Ostrovsky, and M. Titov, Phys. Rev. B **96**, 235148 (2017).
[35] N. Liu, J. Teng, and Y. Li, Nat. Commun. **9**, 1282 (2018).
[36] A. C. Keser, R. Raimondi, and D. Culcer, Phys. Rev. Lett. **123**, 126603 (2019).

[37] S. Yang, Z. Li, C. Lin, C. Yi, Y. Shi, D. Culcer, and Y. Li, Phys. Rev. Lett. **123**, 096601 (2019).
[38] L. A. Yeoh, A. Srinivasan, O. Klochan, R. Winkler, U. Zülicke, M. Y. Simmons, D. A. Ritchie, M. Pepper, and A. R. Hamilton, Phys. Rev. Lett. **113**, 236401 (2014).
[39] T. Li and O. P. Sushkov, Phys. Rev. B **94**, 155311 (2016).
[40] F. Nichele, S. Chesi, S. Hennel, A. Wittmann, C. Gerl, W. Wegscheider, D. Loss, T. Ihn, and K. Ensslin, Phys. Rev. Lett. **113**, 046801 (2014).
[41] F. Nichele, A. N. Pal, R. Winkler, C. Gerl, W. Wegscheider, T. Ihn, and K. Ensslin, Phys. Rev. B **89**, 081306(R) (2014).
[42] M. Brauns, J. Ridderbos, A. Li, E. P. A. M. Bakkers, W. G. van der Wiel, and F. A. Zwanenburg, Phys. Rev. B **94**, 041411(R) (2016).
[43] M. Brauns, J. Ridderbos, A. Li, W. G. van der Wiel, E. P. A. M. Bakkers, and F. A. Zwanenburg, Appl. Phys. Lett. **109**, 143113 (2016).
[44] D. Q. Wang, O. Klochan, J.-T. Hung, D. Culcer, I. Farrer, D. A. Ritchie, and A. R. Hamilton, Nano Lett. **16**, 7685 (2016).
[45] G. Akhgar, O. Klochan, L. H. Willems van Beveren, M. T. Edmonds, F. Maier, B. J. Spencer, J. C. McCallum, L. Ley, A. R. Hamilton, and C. I. Pakes, Nano Lett. **16**, 3768 (2016).
[46] F. Qu, J. van Veen, F. K. de Vries, A. J. A. Beukman, M. Wimmer, W. Yi, A. A. Kiselev, B.-M. Nguyen, M. Sokolich, M. J. Manfra, F. Nichele, C. M. Marcus, and L. P. Kouwenhoven, Nano Lett. **16**, 7509 (2016).
[47] F. Nichele, M. Kjaergaard, H. J. Suominen, R. Skolasinski, M. Wimmer, B.-M. Nguyen, A. A. Kiselev, W. Yi, M. Sokolich, M. J. Manfra, F. Qu, A. J. A. Beukman, L. P. Kouwenhoven, and C. M. Marcus, Phys. Rev. Lett. **118**, 016801 (2017).
[48] A. Srinivasan, D. S. Miserev, K. L. Hudson, O. Klochan, K. Muraki, Y. Hirayama, D. Reuter, A. D. Wieck, O. P. Sushkov, and A. R. Hamilton, Phys. Rev. Lett. **118**, 146801 (2017).
[49] S. Conesa-Boj, A. Li, S. Koelling, M. Brauns, J. Ridderbos, T. T. Nguyen, M. A. Verheijen, P. M. Koenraad, F. A. Zwanenburg, and E. P. A. M. Bakkers, Nano Lett. **17**, 2259 (2017).
[50] S.-X. Li, Y. Li, F. Gao, G. Xu, H.-O. Li, G. Cao, M. Xiao, T. Wang, J.-J. Zhang, and G.-P. Guo, Appl. Phys. Lett. **110**, 133105 (2017).
[51] Y. Li, S.-X. Li, F. Gao, H.-O. Li, G. Xu, K. Wang, D. Liu, G. Cao, M. Xiao, T. Wang, J.-J. Zhang, G.-C. Guo, and G.-P. Guo, Nano Lett. **18**, 2091 (2018).
[52] L. Vukusic, J. Kukucka, H. Watzinger, J. M. Milem, F. Schaffler, and G. Katsaros, Nano Lett. **18**, 7141 (2018).
[53] S. Liles, R. Li, C. H. Yang, F. E. Hudson, M. Veldhorst, A. S. Dzurak, and A. R. Hamilton, Nat. Commun. **9**, 3255 (2018).
[54] N. W. Hendrickx, D. P. Franke, A. Sammak, M. Kouwenhoven, D. Sabbagh, L. Yeoh, R. Li, M. L. V. Tagliaferri, M. Virgilio, G. Capellini, G. Scappucci, and M. Veldhorst, Nat. Commun. **9**, 2835 (2018).
[55] A. Crippa, R. Maurand, L. Bourdet, D. Kotekar-Patil, A. Amisse, X. Jehl, M. Sanquer, R. Lavieville, H. Bohuslavskyi, L. Hutin, S. Barraud, M. Vinet, Y.-M. Niquet, and S. De Franceschi, Phys. Rev. Lett. **120**, 137702 (2018).
[56] N. W. Hendrickx, W. I. L. Lawrie, L. Petit, A. Sammak, G. Scappucci, and M. Veldhorst, Nat. Commun. **11**, 3478 (2020).
[57] M. Marx, A. G. Jun Yoneda, P. Stano, T. Otsuka, K. Takeda, S. Li, Y. Yamaoka, T. Nakajima, A. Noiri, D. Loss, T. Kodera, and S. Tarucha, arXiv:2003.07079.
[58] C. Kloeffel, M. Trif, P. Stano, and D. Loss, Phys. Rev. B **88**, 241405(R) (2013).
[59] Y.-P. Shim and C. Tahan, Nat. Commun. **5**, 4225 (2014).
[60] J.-T. Hung, E. Marcellina, B. Wang, A. R. Hamilton, and D. Culcer, Phys. Rev. B **95**, 195316 (2017).
[61] R. Moriya, K. Sawano, Y. Hoshi, S. Masubuchi, Y. Shiraki, A. Wild, C. Neumann, G. Abstreiter, D. Bougeard, T. Koga, and T. Machida, Phys. Rev. Lett. **113**, 086601 (2014).
[62] F. Nichele, M. Kjaergaard, H. J. Suominen, R. Skolasinski, M. Wimmer, B.-M. Nguyen, A. A. Kiselev, W. Yi, M. Sokolich, M. J. Manfra, F. Qu, A. J. A. Beukman, L. P. Kouwenhoven, and C. M. Marcus, Phys. Rev. Lett. **118**, 016801 (2017).
[63] A. J. A. Beukman, F. K. de Vries, J. van Veen, R. Skolasinski, M. Wimmer, F. Qu, D. T. de Vries, B.-M. Nguyen, W. Yi, A. A. Kiselev, M. Sokolich, M. J. Manfra, F. Nichele, C. M. Marcus, and L. P. Kouwenhoven, Phys. Rev. B **96**, 241401(R) (2017).
[64] R. Winkler, D. Culcer, S. J. Papadakis, B. Habib, and M. Shayegan, Semicond. Sci. Technol. **23**, 114017 (2008).
[65] C.-X. Liu, B. Zhou, S.-Q. Shen, and B.-F. Zhu, Phys. Rev. B **77**, 125345 (2008).
[66] S. Chesi, G. F. Giuliani, L. P. Rokhinson, L. N. Pfeiffer, and K. W. West, Phys. Rev. Lett. **106**, 236601 (2011).
[67] A. Scholz, T. Dollinger, P. Wenk, K. Richter, and J. Schliemann, Phys. Rev. B **87**, 085321 (2013).
[68] V. E. Sacksteder and B. A. Bernevig, Phys. Rev. B **89**, 161307(R) (2014).
[69] T. Biswas and T. K. Ghosh, J. Appl. Phys. **115**, 213701 (2014).
[70] A. Mawrie, T. Biswas, and T. K. Ghosh, J. Phys. Condens. Matter **26**, 405301 (2014).
[71] R. Cuan and L. Diago-Cisneros, Europhys. Lett. **110**, 67001 (2015).
[72] J. Fu and J. C. Egues, Phys. Rev. B **91**, 075408 (2015).
[73] T. Biswas, S. Chowdhury, and T. K. Ghosh, Eur. Phys. J. B **88**, 220 (2015).
[74] P. Wenk, M. Kammermeier, and J. Schliemann, Phys. Rev. B **93**, 115312 (2016).
[75] A. Mawrie, S. Verma, and T. K. Ghosh, J. Phys. Condens. Matter **29**, 465303 (2017).
[76] J. Liang and Y. Lyanda-Geller, Phys. Rev. B **95**, 201404(R) (2017).
[77] S. Bladwell and O. P. Sushkov, Phys. Rev. B **99**, 081401(R) (2019).
[78] Y. Liu, A. L. Graninger, S. Hasdemir, M. Shayegan, L. N. Pfeiffer, K. West, K. W. Baldwin, and R. Winkler, Phys. Rev. Lett. **112**, 046804 (2014).
[79] H. Liu, E. Marcellina, A. R. Hamilton, and D. Culcer, Phys. Rev. Lett. **121**, 087701 (2018).
[80] E. Marcellina, A. Srinivasan, D. S. Miserev, O. P. Sushkov, D. Culcer, A. R. Hamilton, A. F. Croxall, D. A. Ritchie, and I. Farrer, Phys. Rev. Lett. **121**, 077701 (2018).

[81] E. Marcellina, P. Bhalla, A. R. Hamilton, and D. Culcer, Phys. Rev. B **101**, 121302(R) (2020).

[82] A. Samanta, D. P. Arovas, and A. Auerbach, Phys. Rev. Lett. **126**, 076603 (2021).

[83] See Supplemental Material at http://link.aps.org/supplemental/10.1103/PhysRevLett.126.256601 for details on the numerical calculations for Figures 1 and 2 and the derivations of equations (3) and (4).

[84] R. Winkler, Phys. Rev. B **62**, 4245 (2000).

[85] R. Winkler, H. Noh, E. Tutuc, and M. Shayegan, Phys. Rev. B **65**, 155303 (2002).

[86] R. Winkler, *Spin-Orbit Coupling Effects in Two-Dimensional Electron and Hole Systems* (Springer, Berlin, 2003).

[87] M. V. Durnev, M. M. Glazov, and E. L. Ivchenko, Phys. Rev. B **89**, 075430 (2014).

[88] E. Marcellina, A. R. Hamilton, R. Winkler, and D. Culcer, Phys. Rev. B **95**, 075305 (2017).

[89] D. S. Miserev and O. P. Sushkov, Phys. Rev. B **95**, 085431 (2017).

[90] D. S. Miserev, A. Srinivasan, O. A. Tkachenko, V. A. Tkachenko, I. Farrer, D. A. Ritchie, A. R. Hamilton, and O. P. Sushkov, Phys. Rev. Lett. **119**, 116803 (2017).

[91] X. Marie, T. Amand, P. LeJeune, M. Paillard, P. Renucci, L. E. Golub, V. D. Dymnikov, and E. L. Ivchenko, Phys. Rev. B **60**, 5811 (1999).

[92] S. J. Papadakis, E. P. De Poortere, H. C. Manoharan, M. Shayegan, and R. Winkler, Science **283**, 2056 (1999).

[93] T. Li, L. A. Yeoh, A. Srinivasan, O. Klochan, D. A. Ritchie, M. Y. Simmons, O. P. Sushkov, and A. R. Hamilton, Phys. Rev. B **93**, 205424 (2016).

[94] X. Bi, P. He, E. M. Hankiewicz, R. Winkler, G. Vignale, and D. Culcer, Phys. Rev. B **88**, 035316 (2013).

[95] F. T. Vasko and O. E. Raichev, *Quantum Kinetic Theory and Applications* (Springer, New York, 2005).